Nucl. Fusion **51** (2011) 113018 (8pp) doi:10.1088/0029-5515/51/11/113018

Transient CHI start-up simulations with the TSC

R. Raman[1], S.C. Jardin[2], J. Menard[2], T.R. Jarboe[1], M. Bell[2], D. Mueller[2], B.A. Nelson[1] and M. Ono[2]

[1] Department of Aeronautics and Astronautics, University of Washington, Seattle, AERB 352250, Seattle, WA, 98195 USA
[2] Princeton Plasma Physics Laboratory, 100 Stellarator Road, Princeton, NJ, 08543 USA

Received 22 February 2011, accepted for publication 30 June 2011
Published 28 October 2011
Online at stacks.iop.org/NF/51/113018

Abstract
Transient coaxial helicity injection (CHI) has been successfully used in the helicity injected torus-II and the National Spherical Torus Experiment (NSTX) for a demonstration of closed-flux current generation without the use of the central solenoid. The Tokamak Simulation Code (TSC) has now been used to understand the scaling of CHI generated toroidal current with variations in the external toroidal field and injector flux. These simulations show favourable scaling of the CHI start-up process with increasing machine size. Closed flux in TSC is achieved as a result of the decaying CHI discharge that induces a positive loop voltage generating the initial closed-flux current.

(Some figures in this article are in colour only in the electronic version)

1. Introduction

The spherical torus (ST) is capable of simultaneous operation at high beta and high bootstrap current fraction [1]. These advantages of the ST configuration arise as a result of its small aspect ratio. At the low aspect ratios needed for an ST reactor, because of the very restricted space for a central solenoid, elimination of the central solenoid is an important requirement. Thus, current generation methods that do not rely on the central solenoid are necessary for the viability of the ST concept. Elimination of the central solenoid could also lead to a more compact tokamak [2]. The National Spherical Torus Experiment (NSTX) is exploring the technique known as transient coaxial helicity injection (CHI) [3] as a method to produce the initial plasma and sufficient toroidal plasma current to allow other methods of non-inductive current drive and sustainment to be applied. The method of CHI has previously been used in spheromaks, in other STs [4–8], and in the large aspect ratio tokamak, DIII-D [9].

CHI is implemented in NSTX by driving current along field lines that connect the inner and outer lower divertor plates (the injector region). For CHI start-up, gas is injected in a cavity below the lower divertor plates and a 5–20 mF capacitor bank charged to 1.75 kV is discharged across the lower divertor plates. If the injector current exceeds a threshold value, the resulting $\Delta B_{\rm tor}^2(J_{\rm pol} \times B_{\rm tor})$ stress across the current layer exceeds the field-line tension of the injector flux which causes the helicity and plasma in the lower divertor region to move into the main torus chamber.

CHI has been successfully used in NSTX for the generation of substantial amounts of closed-flux current [10, 11]. To understand the full potential of CHI for future upgrades to NSTX and its scaling to larger devices that are expected to operate at higher values of the toroidal field we have used the Tokamak Simulation Code (TSC) [12–14] to understand the scaling of CHI with the ST toroidal field and injector flux that are used to generate the CHI discharge. TSC, which is a time-dependent, free-boundary, predictive equilibrium and transport code, uses as input the NSTX vessel geometry and external circuit parameters. These are the first results describing transient CHI simulation with the TSC.

2. Results of transient CHI in the NSTX machine

NSTX is a 0.85 m major radius, 0.65 m minor radius machine with a vessel volume of 30 m^3. Toroidal ceramic breaks at the top and bottom of the stainless-steel vessel allowing the inner and outer components of the vessel to be electrically biased enabling CHI operation. The lower divertor region where the discharge originates is referred to as the injector region. The upper divertor region is referred to as an absorber because the $E \times B$ flow that arises as a consequence of voltage application across the inner and outer divertor plates is away from the injector region and into the absorber region.

As shown in figure 1, a transient CHI discharge is produced in NSTX by first energizing the poloidal field (PF) coils near the lower divertor plates to generate field lines that connect the lower inner and outer coaxial rings of the divertor plates. In NSTX these lower divertor plates are electrically insulated from each other and serve as electrodes. A pre-programmed amount of gas is then injected in a chamber

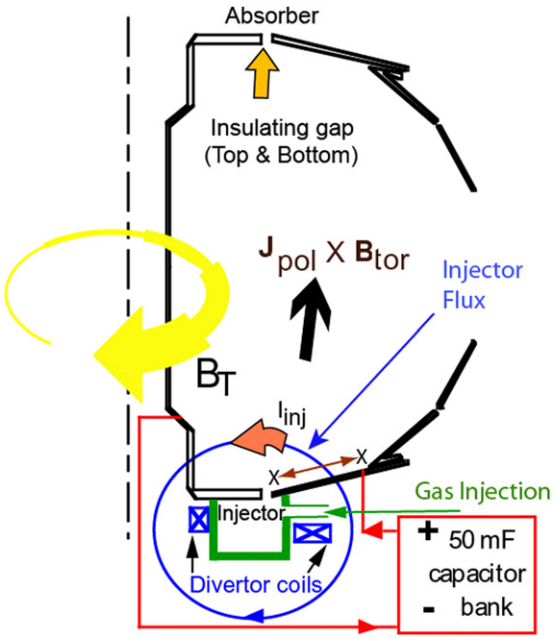

Figure 1. Cartoon drawing of the NSTX machine components including the location of the insulating gaps between the divertor plates, the lower divertor coils used for generating the CHI injector flux and the absorber PF coils.

below these lower divertor plates. As the injected gas emerges through the toroidal gap between the divertor plates, a capacitor bank (5–25 mF typically at 1.7 kV) is connected across the electrodes. The gas breaks down and current begins to flow along the field lines from the outer to the inner divertor plate. If the magnitude of the injected current remains below a threshold, then the open field-line structure will remain close to the lower divertor plates. However, as the injector current increases, the electromagnetic $J_{\rm pol} \times B_{\rm tor}$ force resulting from the current flowing along the PF, overcomes the field-line tension and the open field lines begin to extend into the vacuum vessel. The current required to satisfy this 'bubble burst' condition is given by the relation

$$I_{\rm inj} = 2\psi_{\rm inj}^2/(\mu_0^2 d^2 I_{\rm TF}). \quad (1)$$

Here $\psi_{\rm inj}$ is the poloidal flux at the injector insulating gap and is referred to as the injector flux. It is usually measured as the difference in poloidal flux between two poloidal flux loops at the lower outer divertor plate, as indicated in figure 1 by the letter 'x' separated by the arrow. It is the amount of poloidal flux, generated by the divertor coils, which penetrates the lower outer divertor plate or the lower inner divertor plate. $I_{\rm TF}$ is the total current in the toroidal field coil and d is the width of injector flux 'footprint' on the electrodes [15–17].

As a consequence of the relatively strong toroidal field compared with the PF, the current on the open field lines has a strong toroidal component. On NSTX the magnitude of the generated toroidal plasma current during CHI is typically 50–70 times the magnitude of the injected current (the electrode discharge current), and some discharges have shown current multiplication factors as high as 100 [10]. After the plasma fully fills the vessel, if the injector current is then rapidly reduced, the plasma disconnects from the injector forming a closed field-line configuration which retains a significant toroidal current. If the expanding CHI-produced plasma reaches the (upper) absorber structure while voltage is still being applied across the electrodes, a secondary discharge can develop in the absorber. This is referred to as an 'absorber arc' and it can present a much lower impedance than the injector. In the earlier *driven* CHI experiments on NSTX [18], soon after an absorber arc was produced nearly all of the injected current would flow through the arc in the upper portion of the machine and an insufficient amount of current would flow through the main plasma load, so the driven CHI effect was lost. In the more recent transient CHI approach, if the arc is not too severe, the CHI discharge itself continues to be driven, but there is now an influx of low-Z impurities into the plasma that degrades the plasma quality. In this case the CHI effect is not lost but the plasma quality is degraded.

The CHI method drives current initially on open field lines creating a current density profile in the poloidal (R–Z) plane that is hollow. Taylor relaxation predicts a flattening of this current profile leading to current being driven throughout the volume. Current penetration to the interior is needed for usefully coupling CHI to other current drive methods and to provide CHI-produced sustainment current during an extended non-inductive phase.

CHI can be applied in two ways. In both methods, the toroidal plasma current produced by CHI initially flows on open field lines joining the electrodes. In order to produce toroidal plasma current on closed-flux surfaces magnetic reconnection must occur. In the first approach referred to as *the steady state* or *driven* CHI, closed-flux generation relies on the development of some form of non-axisymmetric plasma perturbation. This mode of CHI operation, in which the injector circuit is continuously driven for a time longer than the timescale for resistive decay of the toroidal current was initially studied in the early CHI experiments in NSTX [18]. However, for initial plasma start-up it was found in the HIT-II ST that a new mode of CHI operation in an ST, referred to as *transient* CHI [3], which involves only axisymmetric magnetic reconnection works very well and produces useful closed-flux equilibrium. In transient CHI, the initial PF configuration is chosen such that the plasma carrying the injected current rapidly expands into the chamber. When the injected current is rapidly decreased, magnetic reconnection occurs near the injection electrodes, with the toroidal plasma current forming closed-flux surfaces. The method of transient CHI has now been successfully used on NSTX for an unambiguous demonstration of closed-flux current generation without the use of the central solenoid [10]. As described below, we have now used the TSC to simulate the discharge evolution of these transient CHI discharges in NSTX.

We would like to clarify that the purpose of this work is not to obtain detailed agreement with the experiment but rather to understand the CHI-produced toroidal current scaling with toroidal field and injector flux and to compare the results with the predictions of equation (1).

3. Results from TSC simulations

TSC is a time-dependent, free-boundary, predictive equilibrium and transport code [12–14]. It has the ability to aid in

scenario development of both discharge energetics and plasma control systems. It solves fully dynamic MHD/Maxwell's equations coupled to transport and Ohms's law equations. It requires as input the device hardware and coil electrical characteristics, as well as assumptions concerning plasma density profile (or particle diffusivity), impurities and other global discharge characteristics. It models the evolution of free-boundary axisymmetric toroidal plasma on the resistive and energy confinement time scales. The plasma equilibrium and field evolution equations are solved on a two-dimensional Cartesian grid. Boundary conditions between plasma/vacuum/conductors are based on the fact that the poloidal flux and tangential electric field are continuous across interfaces. The circuit equations are solved for all of the PF coil systems with the effects of induced currents in passive conductors included. Open field lines are included, and the halo current is computed as part of the calculation. In this modelling, the NSTX vacuum vessel is modelled as a metallic structure with poloidal breaks at the top and bottom. An electric potential V is applied across the break. For clarification, halo currents are not to be confused with Hiro currents, which are skin currents on closed field lines that are excited by the plasma motion [19]. Halo currents are currents that flow on open field lines connecting the plasma to the vessel. These can be driven by self-induced currents, as occurs during a plasma disruption, or by the application of external voltages as is the case during CHI plasma start-up.

It is important to note that TSC allows for the possibility of reconnection. What it does not have is the capability to model the effects of 3D reconnection activity such as that which would occur during the steady-state CHI approach that relies on non-axisymmetric modes to drive current. TSC solves Ohm's law, which allows for the formation of closed-flux surfaces in the presence of a loop voltage, much as the generation of closed-flux surfaces during transformer current drive. Because a positive inductive voltage is generated during the decay of the CHI injected poloidal flux, part of the injected poloidal flux closes in on itself to produce closed-flux surfaces. Because the transient CHI approach relies primarily on axisymmetric 2D type reconnection, the modelling of these discharges is within the realm of the present equations used in TSC. The fact that TSC is able to obtain these results without accounting for relaxation phenomena, which are much more difficult to simulate, makes it a very useful tool for extending this work to future machines.

Three different sets of simulations have been conducted. For the first case, we have used coil current data from an NSTX discharge to simulate the discharge evolution. For the second case, we have studied the changes to the generated current and the current multiplication factor as both the external toroidal field and the injector poloidal flux is varied. For the final simulation, we have explored the CHI current generation potential in NSTX as the vacuum toroidal field magnitude is increased to the 1 T level, which is the design level for the proposed upgrade to NSTX. These three cases are described in the subsequent sections.

3.1. Simulation of an NSTX discharge

The discharge being simulated is an early NSTX transient CHI discharge that successfully demonstrated current persistence, a condition when the CHI-produced toroidal current persisted after the injector current had been reduced to zero. This was an indicator of a closed-flux equilibrium that was decaying in time. Later, equilibrium reconstructions supported the presence of closed-flux surfaces in such discharges with current persistence [10]. We used the same PF coil currents as were used in NSTX Shot 118340. Due to the difficulty in computing the actual plasma resistance including the plasma-vessel sheath resistance in this case, we did not attempt to use the experimentally measured voltage, but rather applied a voltage V across the lower vessel gap and adjusted this value V to give approximate agreement with the measured toroidal current. In figure 2 we illustrate the results of the TSC calculations of the CHI experimental data shown in figure 2 in [10] and for convenience, part of it is reproduced here in figure 3. About 60 kA of toroidal current is generated soon after current peak, and as in the experiment, at the time of peak toroidal current, the injector current is similar to the experimental value. The poloidal flux plots show the plasma evolves in much the same way as observed experimentally from fast camera images of the plasma growth and there is approximate agreement with the experimental equilibrium reconstruction.

In these simulations the injector voltage is varied by a controller to obtain the required injector current. This is similar to what is done experimentally. The injector current is the parameter that needs to be controlled. This is also reflected in equation (1), which relates the plasma current to the injector current and not to the voltage. For example, experimentally, for identical injector flux conditions in the same machine a different value of the voltage may be required to produce the same injector current since the magnitude of the injector current depends on the resistivity of the plasma and the edge sheath conditions. These depend on many things that are difficult to predict such as the conditioning of the machine, the presence of impurities and the possible presence of auxiliary heating. Experimentally, if we are unable to get the injector current needed to inject a given amount of poloidal injector flux, then we simply increase the voltage to a level that is required to obtain the needed injector current.

The discrepancies between the experimental results shown in figure 3 and the simulated discharges are because the early start-up phase of a CHI discharge is dynamic with reconnection activity and possibly with the presence of non-axisymmetric modes during the driven phase. Because of gas breakdown variations some CHI discharges, such as the one shown in figure 3, sometimes start after some delay after the voltage is applied to the electrodes. These aspects cannot be simulated by TSC. After the injector current is turned off the injected plasma becomes much more quiescent and is similar to inductively generated plasma that is decaying. As a result, TSC cannot accurately reproduce the detailed dynamics of the plasma evolution itself, although as seen from these simulations and in the subsequent sections it does a remarkable job of reproducing the overall macroscopic results related to important scaling parameters such as the scaling with injector flux and toroidal field, which are needed for projecting CHI start-up capability in other machines.

Generation of closed flux in TSC is as a result of an effective toroidal loop voltage induced by the CHI ejected

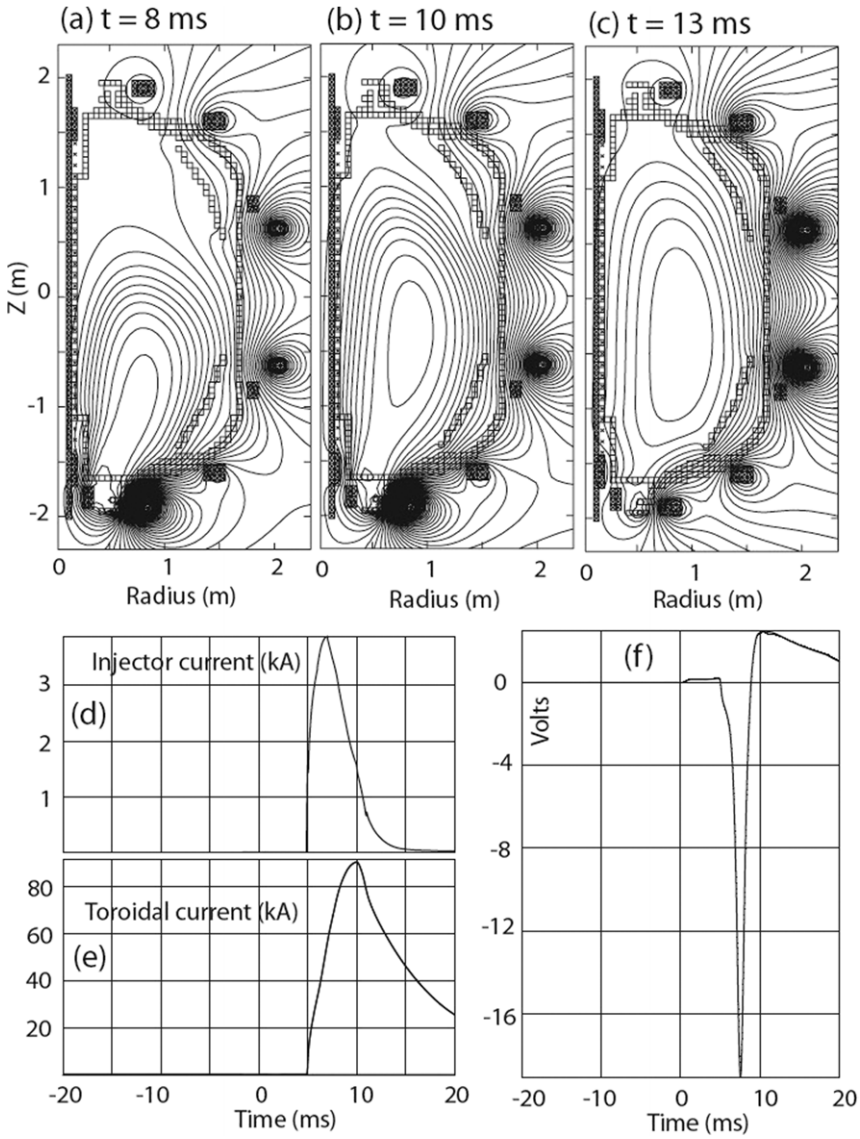

Figure 2. Simulation of a 60 kA NSTX transient CHI discharge (shown in figure 3) with the TSC. For these simulations, the coil currents used in the experiment were used as input parameters. The CHI voltage is applied at 5 ms. Shown are (*a*)–(*c*) poloidal flux contours, (*d*) the injector current, (*e*) the plasma current and (*f*) the induced loop voltage at $Z = -0.3$ m along the inner vessel during the growth and decay of the CHI plasma discharge.

poloidal flux that decreases as the injector current is reduced to zero. This is shown in figure 2(*f*), which is a plot of the induced loop voltage at $Z = -0.3$ m along the inner wall of NSTX. It shows the induction of large negative loop voltage as the plasma grows. The rapid injection of poloidal flux is responsible for the induced negative loop voltage. However, as the plasma begins to decay due to the pre-programmed injector voltage being reduced to zero, a relatively smaller positive loop voltage is induced, and coincident with this, closed-flux surfaces are generated in the discharge. The simulations shown in figure 2 have been run at an electron temperature of 15 eV.

3.1.1. Scaling with toroidal field. Shown in figure 4 is the result of several TSC runs in which the injector flux was maintained constant and the toroidal field was increased. Simulations were run at 0.3, 0.6 and 0.9 T. For each of these cases the applied electric field across the CHI injector gap was sequentially increased until the discharge filled the vessel and began to interact with the absorber region. In figure 4(*a*), the three lower traces correspond to the injector current, and the three upper traces correspond to the CHI-produced toroidal current. The injector current shows an initial change in slope as the voltage is increased. The inflex point of this trace is related to the bubble burst current. Thus as the toroidal field is increased, less injector current is required to satisfy the bubble burst current requirement while a higher voltage is needed to get to the same injector current as for the lower toroidal field case. This indicates that at 1 T, a slightly higher voltage capability may be required on NSTX-U, but probably less than a factor of 2. Additional analysis is needed to establish the voltage requirements for NSTX-U. The simulations also show that at a given injector current the attained toroidal current also increases with the toroidal field. This result is also true for *driven* CHI because *driven* CHI is an extension of the transient

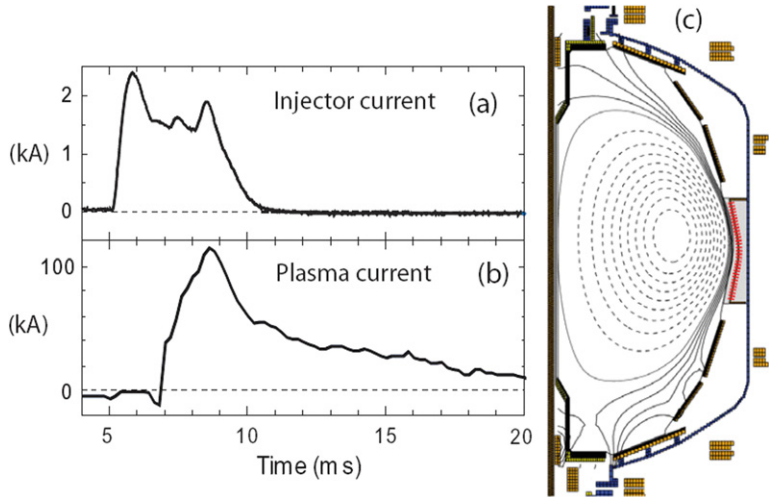

Figure 3. (*a*) Injector current, (*b*) plasma current and (*c*) equilibrium reconstruction for NSTX discharge 118340 at $t = 13$ ms are shown. The discharge was run at a toroidal field of 0.4 T.

CHI case during which the injector current is not reduced after the injector flux fills the vessel. Figure 4(*b*) shows the attained current multiplication for the three toroidal field cases. It shows that the current multiplication significantly increases with toroidal field. The maximum current multiplication factor seen in these discharges is similar to the values achieved experimentally, which varies from 60 to nearly 100 for some discharges. These results for the simulations are qualitatively consistent with the earlier simple model developed by Jarboe [15], which is described by equation (1). Given the resolution of the data points near the inflection point, the inflection point for the 0.9 T case occurs at about 0.65 kA, around 0.95 kA for the 0.6 T case and around 1.85 kA for the 0.3 T case. Because the injector flux magnitude and the flux footprint width are not varied in these simulations, the $1/B_T$ scaling is clearly seen in these TSC simulations. It is seen that the discharge with the highest value of toroidal field does indeed require less injector current. As the toroidal field is increased, the injector impedance increases. This is a consequence of the longer field-line length that has higher resistance, which now requires more voltage to drive a similar magnitude of injector current. Thus for these three cases, as the toroidal field is increased, the injector voltage also needs to be increased to be able to drive an adequate amount of injector current required to satisfy the bubble burst condition.

Results from [15] also show that the attained current multiplication factor should vary as the ratio of the toroidal flux in the vessel to the injected poloidal flux (also referred to as the gun flux or injector flux). To a large extent, this trend is also seen in the TSC simulations. An examination of the highest current multiplication factor attained for the three toroidal field cases shows that after the discharge fully fills the vessel, a condition that is reached at close to the highest value of the applied electric field for each of the cases, the 0.3 T case has a current multiplication factor of about 29, it is 59 for the 0.6 T case and 90 for the 0.9 T case, again reflecting the effect of the toroidal field scaling. What this means for CHI plasma start-up is that machines that have a higher toroidal field or a larger physical plasma volume or both would realize much higher values of the current multiplication factor, an aspect which has also been observed experimentally. The smaller HIT-II machine typically saw current multiplication factors of 6, whereas NSTX, which has ten times more toroidal flux than HIT-II, typically sees a current multiplication factor of about 60.

3.1.2. Scaling with injector flux. The strong scaling with injector flux dependence is shown in figure 5. As in figure 4, the traces in figure 5(*a*) correspond to the injector current and the achieved toroidal current and those in figure 5(*b*) contain the current multiplication factor. The general observation is that the injector current required to cause the injected poloidal flux to fill the vessel is about 2.5 kA for the reference injector flux case, it increases to about 7.5 kA as the injector flux is doubled and further increases to 14 kA as the injector flux is tripled while the toroidal field and flux footprint width are held constant. The injector flux is varied by changing the magnitude of the currents in the lower divertor PF coils (injector coils) that are used to generate flux that connects the inner and outer divertor plates. With increasing injector flux the connection distance between the electrodes decreases, so less voltage is needed to get to a given injector current. The increase in the required injector current, within the resolution of these calculations, scales as the square of the injector flux. The maximum current multiplication factor achieved for the three cases are about 60, 30 and 20, respectively, which again reflect the ratio of the toroidal flux to the injector flux.

The simulations for figures 4–6 have been run at 40 eV, as recent results on NSTX indicate the attainment of 30 eV electron temperatures and so temperatures in the range of 40 eV may be more realistic of what could be obtained as the plasma current is increased. For figures 4 and 5, which show the scaling of the current multiplication factor with toroidal field and injector flux, the plots would remain unchanged if a lower electron temperature is used. For a lower value of the electron temperature, the x-axis which is the applied electric field would be higher by a factor needed to obtain a given injector current.

These results show that to a large extent, TSC can reproduce the discharge electromagnetics related to the amount of poloidal flux injected into the vessel for a given injector current and toroidal field in the device.

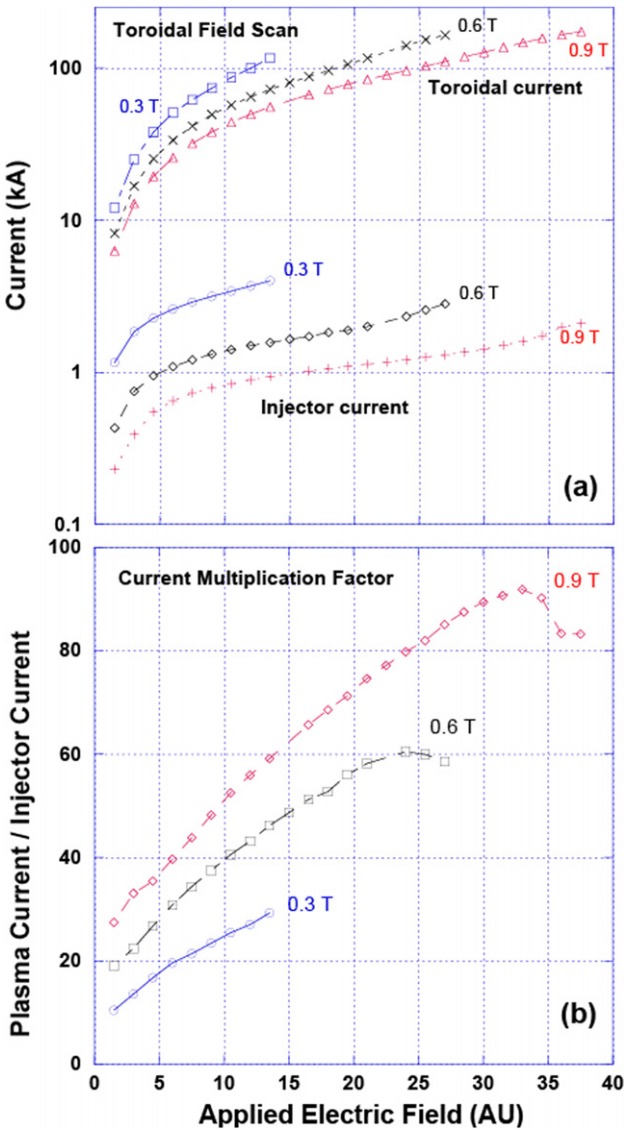

Figure 4. Simulations in which the injector poloidal flux was held constant and the applied voltage varied for three different values of the toroidal field (0.3, 0.6 and 0.9 T). (*a*) Injector current (the lower three traces) and the CHI-produced toroidal current (top three traces) are shown. (*b*) Shown are the current multiplication factors as the toroidal field is varied.

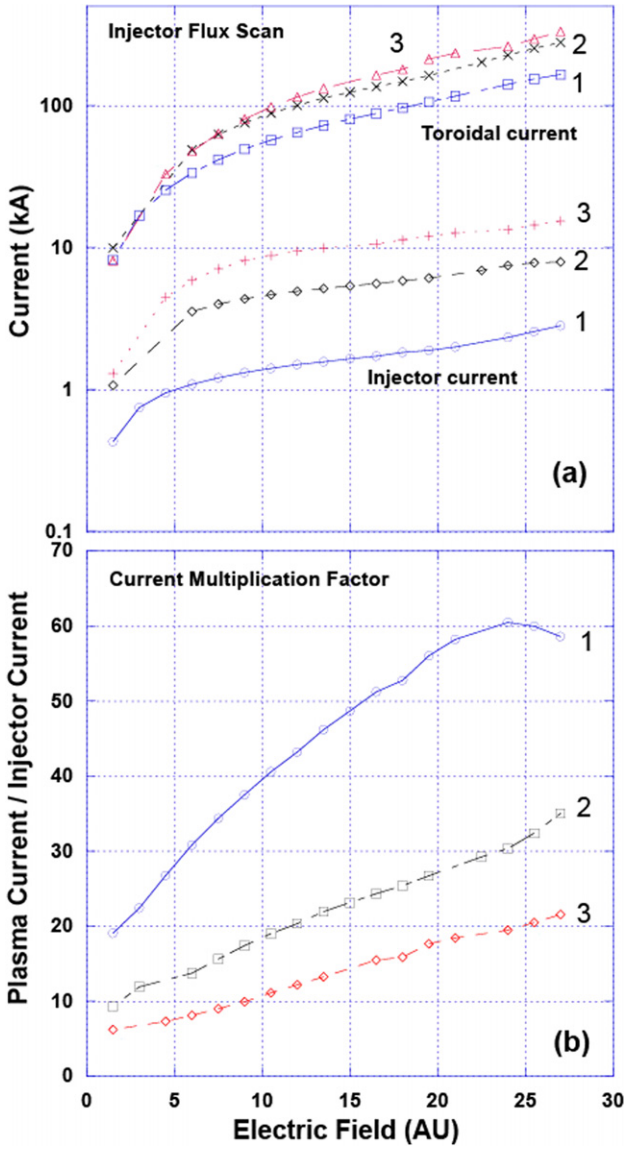

Figure 5. Simulations in which the toroidal field was held constant and the applied voltage varied for three different values of the injector flux. (*a*) Shows the injector current (the lower three traces) and the CHI-produced toroidal current (top three traces). (*b*) Shown are the current multiplication factors as the injector flux is varied.

3.2. Attainable toroidal currents at 1 T

In a simulation run at 1 T toroidal field and with the PF coils programmed to provide equilibrium, it is seen in figure 6 that toroidal currents in excess of 600 kA should be achievable in NSTX if the magnitude of the toroidal field could be increased to 1 T. The need for the higher toroidal field is to reduce the injector current as this places a limit on the useful poloidal flux that could be injected. Doubling the toroidal field allows the same amount of poloidal flux to be injected at half the injector current. The simulations also show that better programming may be required to control the time rate of growth of the CHI discharge. This is done by adjusting the voltage time history. On NSTX, the transient CHI power system is composed of three independently triggered capacitor modules. The size of each of these can be individually controlled. Indeed on NSTX, it was only after implementing this staged capacitor bank capability, to better control the voltage application history that NSTX could achieve high levels closed-flux current generation. The applied voltage time history and the attained current are shown in figures 6(*b*) and (*c*). This indicates that for NSTX, increasing the number of these modules may provide more control over the discharge evolution and better control of the incidence of absorber arcs. For the discharge shown in figure 6(*a*), the electron temperature was restricted to 40 eV throughout the discharge. If during the current decay phase, starting at about 12 ms, the electron temperature is increased to 150 eV, as could be expected from additional heating sources such as from high harmonic fast wave heating or by early neutral beam injection, then the current decay rate substantially slows down as one would expect. This result is shown figure 6(*d*).

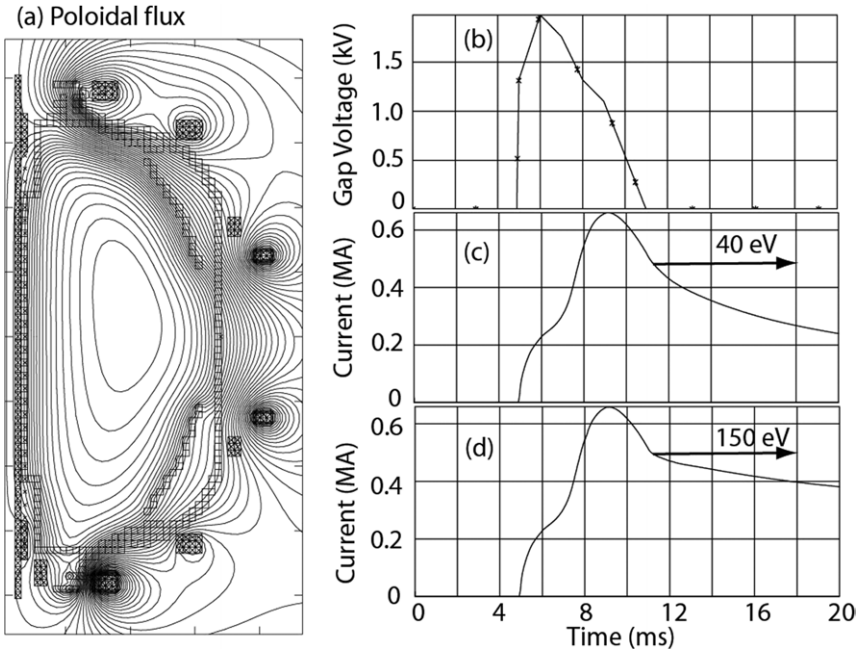

Figure 6. A simulation similar to that shown in figure 2, but with the toroidal field increased to 1 T and the injector flux increased to about 80% of that allowed by the divertor coil current limits in NSTX. Peak toroidal current of 625 kA is generated. The electron temperature throughout the plasma is held at 40 eV and Z_{eff} is 2.5. Shown are (*a*) the poloidal flux contours at 13.5 ms, (*b*) the CHI gap voltage, (*c*) the CHI-produced toroidal current and (*d*) the CHI-produced toroidal current for the case in which the electron temperature is increased to 150 eV for times 12 ms and beyond.

4. Summary

TSC has been able to show consistency with earlier theory [15–17] for the scaling of CHI-produced current with the injector and toroidal fluxes. These results in conjunction with experimental work on HIT-II and NSTX, two machines with different sizes, suggest that the amount of injector current required to inject a given amount of poloidal flux into the vessel increases as the square of the injector flux but decreases with the toroidal field indicating that the scaling to future machines with stronger toroidal field is quite favourable.

Generation of closed flux in TSC is due to an effective toroidal loop voltage induced by the CHI ejected poloidal flux that decreases as the injector current is reduced to zero. Decay of the injected poloidal flux is expected and a natural consequence of the transient CHI processes as the size of the capacitor bank is adjusted so that after the plasma fills the vessel little energy is left in the capacitor bank to meet the bubble burst threshold condition.

Generation of closed flux in TSC is solely a consequence of the induced positive loop voltage. In reality, however, there is a second contributing factor that should make the generation of closed flux easier. This is due to reconnection activity near the injector region, irrespective of the presence of a positive loop voltage inside the containment vessel. In transient CHI discharges, the lower divertor coils are pre-programmed to keep the oppositely directed flux footprints of the poloidal flux on the lower divertor plates close to each other. Because of this there is a tendency for the field lines in this region to naturally reconnect. This aspect of reconnection physics is not modelled in TSC at this time. Nevertheless, TSC results are consistent with many early predictions of the way CHI is expected to work in a ST.

In summary, simulations with the TSC have been found to be consistent with the theoretical model for CHI plasma start-up. However, these simulations now provide a new and powerful capability for optimizing and designing CHI systems in future upgrades to NSTX and to other tokamaks. Results show that for a given injector current closed-flux current generation using transient CHI scales with increased toroidal flux in the vessel. This is a parameter that is expected to increase in future STs that will have a higher toroidal field and a larger plasma cross-section. As a result of higher current multiplication, the required injector current decreases. This is an important result as the reduced injector current translates to a more efficient system and also due to reduced interactions with the electrodes. Additionally, the simulations also show that at fixed injector current the total CHI generated current can be increased by increasing both the toroidal field and the injector flux.

The implications of these scaling results are quite favourable to a larger ST which is projected to operate at toroidal fields of up to 2.5 T. At the expected level of start-up current in these devices, other well-established non-inductive current drive methods, such as the neutral beam current drive and radio frequency current drive could ramp the CHI started current to the levels required for steady-state operation.

Acknowledgment

This manuscript has been authored by Princeton University and collaborators under contract numbers DE-AC02-09CH11466 and DE-FG02-99ER54519 AM08 with the US Department of Energy.

References

[1] Ono M. *et al* 2000 *Nucl. Fusion* **40** 557
[2] Najmabadi F. and the ARIES Team 1998 *Fusion Eng. Des.* **41** 365
[3] Raman R. *et al* 2003 *Phys. Rev. Lett.* **90** 075005
[4] Jarboe T.R. and Alper B. 1987 *Phys. Fluids* **30** 1177
[5] McLean H.S. *et al* 2002 *Phys. Rev. Lett.* **88** 125004
[6] Nelson B.A. *et al* 1995 *Phys. Plasmas* **2** 2337
[7] Nagata M., Kanki T., Fukumoto N. and Uyama T. 2003 *Phys. Plasmas* **10** 2932
[8] Browning P.K. *et al* 1992 *Phys. Rev. Lett.* **68** 1722
[9] Mahdavi M.A. *et al* 1991 IAEA-CN-53/A-IV-7 *Proc. Plasma Physics and Controlled Nuclear Fusion Research (Washington, DC)* vol 1 (Vienna: IAEA) p 335
[10] Raman R. *et al* 2006 *Phys. Rev. Lett.* **97** 175002
[11] Raman R. *et al* 2007 *Phys. Plasmas* **14** 056106
[12] Jardin S.C., Pomphrey N. and Delucia J. 1986 *J. Comput. Phys.* **66** 481–507
[13] Jardin S.C., Bell M.G. and Pomphrey N. 1993 *Nucl. Fusion* **33** 371
[14] Jardin S.C. and Park W. 1981 *Phys. Fluids* **24** 679
[15] Jarboe T.R. 1989 *Fusion Technol.* **15** 7
[16] Redd A.J. *et al* 2008 *Phys. Plasmas* **15** 022506
[17] Redd A.J. *et al* 2007 *Phys. Plasmas* **14** 112511
[18] Raman R. *et al* 2001 *Nucl. Fusion* **41** 1081
[19] Zakharov L. 2008 *Phys. Plasmas* **15** 062507